

Intramolecular Asymmetric Heck Reactions: Evidence for Dynamic Kinetic Resolution Effects

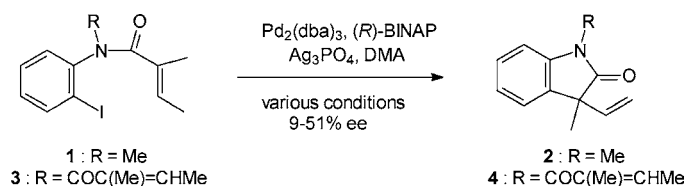
Michael C. McDermott,[†] G. Richard Stephenson,^{*,†} David L. Hughes,[†] and Andrew J. Walkington[‡]

Wolfson Materials and Catalysis Centre, School of Chemical Sciences and Pharmacy, University of East Anglia, Norwich, NR4 7TJ, U.K., and GlaxoSmithKline, Medicines Research Centre, Gunnels Wood Road, Stevenage, Hertfordshire SG1 2NY, U.K.

g.r.stephenson@uea.ac.uk

Received March 13, 2006 (Revised Manuscript Received May 10, 2006)

ABSTRACT



Enantioselectivity of the cyclization of **1** varies at different stages in the reaction. X-ray crystallography has shown that **1** exists as enantiomerically pure (*M*) and (*P*) chiral helical structures defined by the relative orientations of the arene, amide, and alkene. The relative rates of interconversion of the rotamers of **1** have been established, leading to mechanistic proposals to account for the variation of ee based on kinetic resolution effects.

The Heck reaction¹ has become one of the most industrially important and widely used palladium-catalyzed carbon–carbon bond forming reactions. The scope and capabilities of this process have been extensively reviewed.² Asymmetric modification³ has made available a powerful procedure for

the induction of asymmetry in the reactions of aryl iodides and triflates with alkenes, typically involving discrimination between pairs of prochiral enantiotopic alkenes or the enantiofaces of prochiral alkenes and dienes.

An unusual example of the asymmetric Heck reaction was reported by Overman's group⁴ as part of the natural product synthesis of gelsemine. They found that by using a catalyst prepared from Pd₂(dba)₃ and (*R*)-BINAP the addition of triethylamine gave one diastereoisomer of the product, whereas addition of Ag₃PO₄ gave the opposite stereoisomer. Overman's group also demonstrated⁵ that this switch in stereoselectivity could be employed as an enantioselective procedure. In the cyclization of substrate **1** with (*R*)-BINAP as the chiral auxiliary, the use of PMP⁶ as the base gave the (*R*)-(+)-enantiomer of product **2** in 25% ee and the use of

[†] University of East Anglia.

[‡] GlaxoSmithKline U.K.

(1) Heck, R. F. *J. Am. Chem. Soc.* **1968**, *90*, 5518–5526. Dieck, H. A.; Heck, R. F. *J. Am. Chem. Soc.* **1974**, *96*, 1133–1136.

(2) Heck, R. F. *Organic Reactions*; Dauben, W. G., Ed.; Wiley and Sons Inc.: New York, 1982; Vol. 27, Chapter 2, pp 345–390. Trost, B. M.; Verhoeven, T. R. *Comprehensive Organometallic Chemistry*; Abel, E. W., Stone, F. G. A., Wilkinson, G., Eds.; Pergamon Press: Oxford, 1982; Vol. 8, Chapter 57, pp 854–883. Heck, R. F. *Comprehensive Organic Synthesis*; Fleming, I., Semmelhack, M. F., Trost, B. M., Eds.; Pergamon Press: Oxford, 1991; Vol. 4, Chapter 4.3, pp 833–863. Beletskaya, I. P.; Cheprakov, A. V. *Chem. Rev.* **2000**, *100*, 3009–3066.

(3) de Meijere, A.; Meyer, F. E. *Angew. Chem., Int. Ed. Engl.* **1994**, *33*, 2379–2411. Boden, C. D. J.; Kojima, A.; Shibasaki, M. *Tetrahedron* **1997**, *53*, 7371–7395. Shibasaki, M.; Vogl, E. M. *J. Organomet. Chem.* **1999**, *576*, 1–15. Hayashi, M.; Keenan, M.; Loiseleur, O.; Pfaltz, A.; Schmees, N. *J. Organomet. Chem.* **1999**, *576*, 16–22. Dounay, A. B.; Overman, L. E. *Chem. Rev.* **2003**, *103*, 2945–2963. Ohshima, T.; Shibasaki, M.; Vogl, E. M. *Adv. Synth. Catal.* **2004**, *346*, 1533–1552. Bell, H. P.; Ila, H.; Tietze, L. F. *Chem. Rev.* **2004**, *104*, 3453–3516. Guiry, P. J.; McManus, H. A. *Chem. Rev.* **2004**, *104*, 4151–4202.

(4) Mandin, A.; Overman, L. E. *Tetrahedron Lett.* **1992**, *33*, 4859–4862.

(5) Ashimori, A.; Overman, L. E. *J. Org. Chem.* **1992**, *57*, 4571–4572. Ashimori, A.; Matsuura, T.; Overman, L. E.; Poon, D. J. *J. Org. Chem.* **1993**, *58*, 6949–6951. Ashimori, A.; Bachand, B.; Calter, M. A.; Govek, S. P.; Overman, L. E.; Poon, D. J. *J. Am. Chem. Soc.* **1998**, *120*, 6488–6499.

(6) 1,2,2,6,6-Pentamethylpiperidine.

Ag₃PO₄ gave the (*S*)-(-) enantiomer in 59% ee, both in high yields (88–91%).⁷

Our interest in these asymmetric Heck reactions arose from investigations of the use of chiral additives to optimize enantioselectivity⁸ because the factors that controlled enantioselectivity during the asymmetric cyclization were finely balanced, thus changes in reaction conditions and/or the use of additives could profoundly influence the outcome of the reaction.

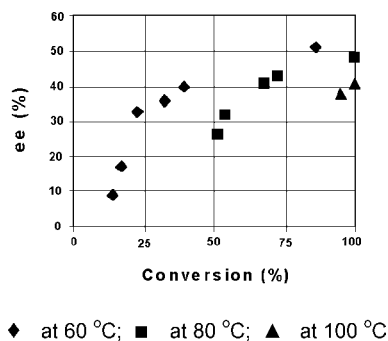
We report here preliminary results from a series of experiments conducted using an Anachem SK233 workstation⁹ equipped with “in-line” chiral HPLC analysis (adapted from an Agilent 1100 HPLC system), in which reaction times, temperatures, concentrations, and catalyst/Ag₃PO₄ loadings were varied (Table 1). The data obtained demon-

(entry 1), the ee of the product **2** was only 9%, but this rose to 40% ee after 240 min (entry 3). Similarly, at 80 °C, an ee of 26% at 60 min (entry 9) improved to 48% ee after 180 min (entry 11). The better high-limit enantioselectivity in this case is ascribed to the more efficient reaction at this temperature (the reaction had gone to completion after 180 min). In general, the data in Table 1 showed that the observed ee of the product is best at high conversions (86–100%) but never reaches the desired high levels of optical purity because of the low ee product accumulated at the early stages of the reaction. At 100 °C (entries 12 and 13), the enantioselectivity is lower than that at 60 °C (entry 5) and at 80 °C (entries 8, 10, and 11), although the reactions at 100 °C were taken more quickly to completion.

Despite the wide range of reaction conditions used in our study, Table 1 (graph) clearly shows that there is a general tendency for high ee's in the product at high conversions and relatively low ee's at low conversions. These data are consistent with the presence of two competing influences. The limiting ee's at 100 °C are ascribed to catalyst decomposition, which is a well-known occurrence in Heck coupling.¹⁰ The reaction mixtures blacken noticeably at this temperature, and if catalytically active Pd(0) particles¹¹ are generated by the thermal decomposition of the Pd(dba)[(*R*)-BINAP] intermediates, a competing racemic cyclization will build up over time. The low ee's observed at lower temperatures at the 60 min stage suggest the presence of a more complex reaction system than a simple kinetic control based on two competing pro-(*R*) and pro-(*S*) mechanisms. In all the examples presented in Table 1, Ag₃PO₄ was used as the base, and the expected (*S*)-(-) product was obtained.¹² Despite the possibility of competing *rac* and pro-(*R*) pathways, the overall asymmetric induction in our examples is consistent with published results^{5,7} on this cyclization reaction.

In an attempt to gain insight into the transition states in the coupling process, the substrate **1** was crystallized from a 3:1 mixture of hexane and DCM and studied by X-ray diffraction. The structure (**5**, Figure 1) takes on a helical form with the bulky *ortho*-iodide substituent on the aromatic ring forcing rotation about the C(2)–N(2) bond by 117°. ¹³ The amide group itself was found to adopt the expected *E*^{14–16} conformation, with considerable pyramidalization of the nitrogen and a C(2)–C(22) torsion angle of 18°. ¹⁷ The adjacent carbon–carbon double bond showed a dihedral

Table 1. Asymmetric Cyclizations of **1** under a Variety of Conditions



entry	temp (°C)	time (min)	catalyst		concn ^a (g mL ⁻¹)	conversion ^b (%)	ee ^c (%)
			loading (mol %)	Ag ₃ PO ₄ (equiv)			
1	60	60	10	5/3	0.2	14	9
2	60	150	10	5/3	0.2	32	36
3	60	240	10	5/3	0.2	39	40
4	60	240	5	5/3	0.2	23	33
5	60	240	5	1/3	0.2	86	51
6	60	240	5	1/3	0.2	17	17
7	80	60	5	2	0.1	54	32
8	80	60	5	2	0.1	68	41
9	80	60	7.5	1	0.08	51	26
10	80	100	7.5	1	0.08	73	43
11	80	180	7.5	1	0.08	100	48
12	100	60	5	5/3	0.2	95	38
13	100	60	10	1/3	0.2	100	41

^a Concentration of **1**. ^b Measured by HPLC. ^c Determined by chiral HPLC using a chiracel OJ column.

strated that the enantioselectivity of the product changes as the reaction proceeds. For example, at 60 °C after 60 min

(7) Ashimori, A.; Matsuura, T.; Overman, L. E.; Poon, D. J. *J. Am. Chem. Soc.* **1998**, *120*, 6477–6487.

(8) Sellarajah, S. Ph.D. Thesis, University of East Anglia, 2001. Sellarajah, S.; Stephenson, G. R. Unpublished results.

(9) Armitage, M. A.; Smith, G. E.; Veal, K. T. *Org. Process Res. Dev.* **1999**, *3*, 189–195. Harre, M.; Tilstam, U.; Weinmann, H. *Org. Process Res. Dev.* **1999**, *3*, 304–318. Information available from www.reactarray.com.

(10) van Leeuwen, P. W. N. M. *Appl. Catal., A Gen.* **2001**, *212*, 61–81. Koningsberger, D. C.; Sietsma, J. R. A.; Tromp, M.; van der Eerden, A. M. J.; van Haaren, R. J.; van Leeuwen, P. W. N. M. *J. Chem. Soc., Chem. Commun.* **2003**, 128–129.

(11) Breinbauer, R.; Reetz, M. T.; Wanninger, K. *Tetrahedron Lett.* **1996**, *37*, 4499–4502. Reetz, M. T.; Westermann, K. *Angew. Chem., Int. Ed.* **2000**, *39*, 165–168.

(12) It is important that Ag₃PO₄ purchased from Aldrich is used.

(13) C(1)–C(21) torsion angle: (+)-anticlinal, 117°.

(14) Chupp, J. P.; Olin, J. F. *J. Org. Chem.* **1967**, *32*, 2297–2303. Curtis, E.; Mislow, K.; Raban, M.; Shvo, Y. *J. Am. Chem. Soc.* **1967**, *89*, 4910–4917. Itai, A.; Saito, S.; Tomioka, N.; Toriumi, Y. *J. Org. Chem.* **1995**, *60*, 4715–4720.

(15) Siddal, T. H.; Stewart, W. E. *Chem. Rev.* **1970**, *70*, 517–551.

(16) Balog, H.; Cass, Q. B.; Curran, D. P.; Degani, A. L. G.; Freitas, L. C. G.; Grieb, S. J.; Hale, G. R.; Hernandez, M. Z. *Tetrahedron: Asymmetry* **1997**, *8*, 3955–3975.

(17) C(2)–C(22) torsion angle: (-)-synclinal, -18°.

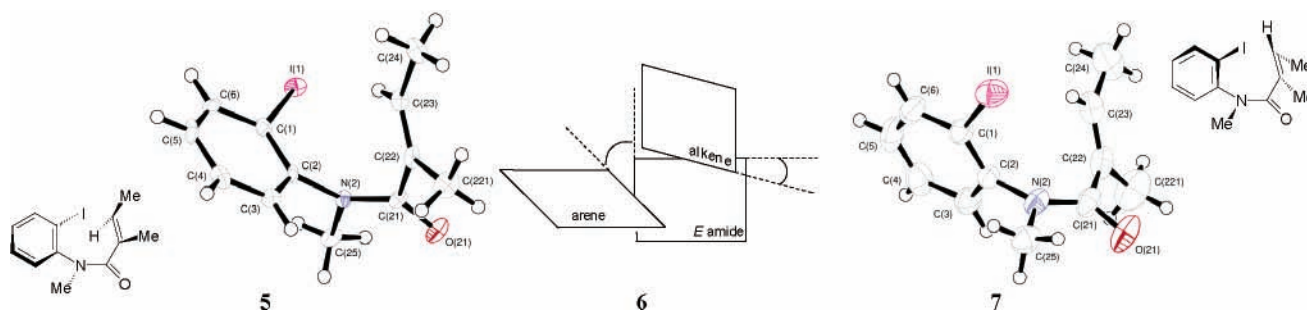


Figure 1. X-ray structure of (*P*)-**1** (**5**), representative arrangement of principal planes (**6**) in (*P*)-**1**, and X-ray structure of (*M*)-**1** (**7**).

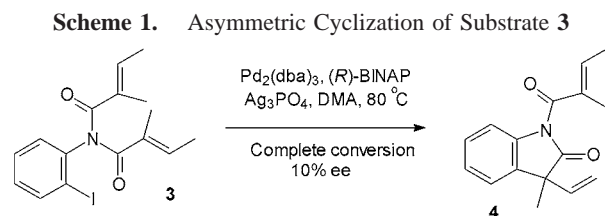
angle of 51° with the amide plane.¹⁸ This structure can be characterized on the basis of three principal planes (**6**, Figure 1), with the overall (*P*) helical form arising from the sequence of (*P*)-axial chirality¹⁹ about the aryl–nitrogen bond [C(2)–N(2)] and also about the carbonyl–alkene [C(21)–C(22)] bond.

The crystal proved to contain a single enantiomer of this (*P*)-helical structure (**5**, Figure 1). A second crystal from the sample yielded a structure of the enantiomeric (*M*)-helical form (**7**, Figure 1).²⁰ The presence of pure (*P*) and (*M*) crystals in solid samples of the starting material for the cyclization (**1**) offers a possible explanation of the anomalous low ee's observed at low conversion because, with the chiral helical conformations of the aryl iodide, a form of kinetic resolution may be in operation.

The 400 MHz ^1H NMR spectra of **1** gave support to the possibility that the helical conformations observed in the solid state are also significant in solution because the signals from the alkene hydrogen and methyls of the 2-methylbut-2-enyl group were broadened suggesting hindered rotation on the NMR timescale. To explore this further, a variable-temperature NMR study of **1** was performed in $\text{DMF-}d_7$ at temperatures between -20 and $+80^\circ\text{C}$, in steps of 5°C . At the low-temperature limit, two distinct signals for the alkene hydrogen were observed at 5.94. and 5.64 ppm in a ratio of ca. 1:9. On the basis of peak assignments^{15,16} for other amide conformers, the more upfield and much larger peak at 5.64 ppm was identified as the *E*-amide. The preference for the *E*-amide in solution,¹⁶ and in the solid state,^{21,22} is well established, further supporting these assignments. The rotational barrier for this dynamic process was estimated as 55 kJ mol^{-1} . Comparison of the two signals observed at -20

$^\circ\text{C}$ shows a difference in rotational broadening indicating the existence of a second dynamic process with a much lower rotational barrier. Compared to these two processes, there is no evidence from the spectroscopic data to establish the relative ease of rotation about the aryl–nitrogen bond [C(2)–N(2)]. Fortunately, evidence in the literature^{16,22,23} allows this issue to be resolved, as there are many reports of configurationally stable amide atropisomers and it is known²⁴ that this may be significant in the control of intramolecular Heck reactions. The interconversion of atropisomers of **1**, although probably accessible at 80°C , will be far slower than the rotations studied in the variable-temperature NMR experiment. Because the atropisomer interconversion is slow and the *E/Z* interconversion is known to be the main process revealed by the NMR study, the third dynamic process must arise from rotation about the carbonyl–alkene bond.

To remove the atropisomer issue, a preliminary series of experiments have been performed employing a symmetrization approach. Using the modified substrate **3**, which contained two 2-methylbut-2-enyl groups as an imide derivative of 2-iodoaniline, the asymmetric Heck reaction (Scheme 1) gave product **4** with an ee of only 10% (measured using



chiral shift NMR experiments^{7,8}), suggesting that the atropisomeric chiral form of **1** may be a significant factor for an efficient asymmetric induction in the Heck cyclization.

(18) N(2)–C(23) torsion angle: (–)-synclinal, -51° .

(19) Cahn, R. S.; Ingold, C. K.; Prelog, V. *Angew. Chem.* **1966**, *78*, 413–447. Cahn, R. S.; Ingold, C. K.; Prelog, V. *Angew. Chem., Int. Ed. Engl.* **1966**, *5*, 385–415, 511.

(20) The chirality of these structures and the *E/Z* form of the amide can be defined by the sequence of torsion angles C(1)–C(21), C(2)–C(22), and N(2)–C(23): (*P*)-**1** +117, –18, -51 [(+)-anticlinal, (–)-synperiplanar, (–)-synclinal]; (*M*)-**1** –117, +16, $+53$ [(–)-anticlinal, (+)-synperiplanar, (+)-synclinal]. The enantiomeric nature of these two helical structures is apparent from the reversal of signs in all three angles, comparing (*P*) and (*M*) forms.

(21) Pedersen, B. F. *Acta Chem. Scand.* **1967**, *21*, 1415–1424. Itai, A.; Kagechika, H.; Saito, S.; Shudo, K.; Toriumi, Y. *J. Am. Chem. Soc.* **1992**, *114*, 10649–10650.

(22) Ates, A.; Curran, D. P. *J. Am. Chem. Soc.* **2001**, *123*, 5130–5131.

(23) Izawa, H.; Kitagawa, O.; Taguchi, T. *Tetrahedron Lett.* **1997**, *38*, 4447–4450. Fushimi, Y.; Kitagawa, O.; Momose, S.; Taguchi, T. *Tetrahedron Lett.* **1999**, *40*, 8827–8831. Bennett, D. J.; Blake, A. J.; Cooke, P. A.; Godfrey, C. R. A.; Pickering, P. L.; Simpkins, N. S.; Walker, M. D.; Wilson, C. *Tetrahedron* **2004**, *60*, 4491–4511. Hata, T.; Kamikawa, K.; Koide, H.; Uemura, M.; Yoshihara, K. *Tetrahedron* **2004**, *60*, 4527–4541. Curran, D. P.; Geib, S. J.; Petit, M. *Tetrahedron* **2004**, *60*, 7543–7552.

(24) Chen, C. H.-T.; Curran, D. P.; Liu, W. *J. Am. Chem. Soc.* **1999**, *121*, 11012–11013.

The X-ray structure of **3** showed disorder of the iodoarene group in the crystal. This group lies in one of two coplanar, overlapping orientations which are shown separately in Figure 2. There were notable differences compared to the

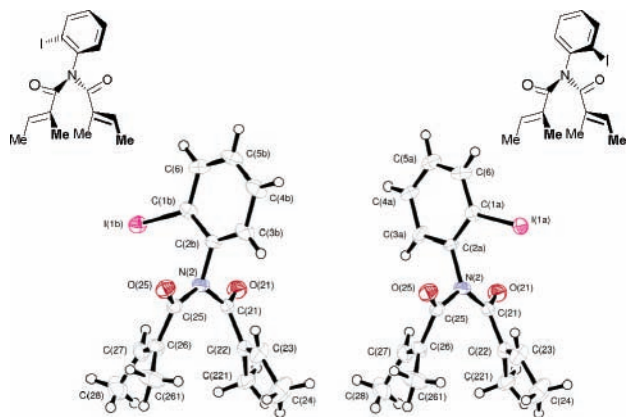


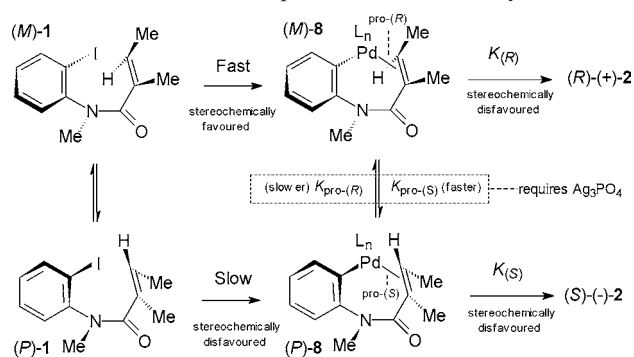
Figure 2. Two structures found in the unit cell of substrate **3**.

structure defined for **1**, with both amide moieties in the imide showing the opposite conformation.²⁵ As expected, the two imide C–N bonds were far longer (1.405 and 1.413 Å) than the amide bond length in **1** (1.361 Å), reducing steric effects in this part of the molecule. The long bond length in the solid state is also presumably present as a true structural feature in solution, as indicated by sharp NMR signals that suggest lowered rotational barriers. The two imide structures observed in the solid state (Figure 2) should rapidly interconvert in solution by the facile rotation about the C(21)–C(22) and C(25)–C(26) bonds.

In the PMP protocol described by Overman,⁷ the dynamic kinetic resolution of interconverting helical iodides (*P*)-**1** and (*M*)-**1** must favor the oxidative addition to the (*M*)-helix to promote the pro-(*R*) pathway to product **2**. For the Ag₃PO₄ protocol, however, this kinetic resolution cannot account for the variation of ee with degree of conversion unless the opposite stereochemical preference is favored in the carbon–carbon bond forming stages [$K_{(R)}/K_{(S)}$] of the cycle. We propose that the addition of Ag₃PO₄ opens an equilibrium between the palladium-bound oxidative addition complexes of the (*P*)- and (*M*)-helices [(*P*)-/(*M*)-**8**; Scheme 2]. The route to the (*S*)-(-)-**2** product would then be favored if the pro-

(25) As the priority of groups changes, this is still labeled *E*.

Scheme 2. Proposed Reaction Pathways



(*S*) catalytic intermediate is the stereochemically preferred helix for the carbon–carbon bond forming step. When the pro-(*R*)/pro-(*S*) interconversion of organopalladium intermediates is operative, the switch in enantioselectivity arises from the Ag₃PO₄-promoted equilibrium improving access to the otherwise slowly formed oxidative addition product from (*P*)-**1**.

In summary, we have shown that chiral helical conformations of 2-iodoanilide **1** interconvert through internal bond rotations leading to the proposal of a dynamic kinetic resolution mechanism to account for the switch of enantioselectivity.

Acknowledgment. We thank the EPSRC (CASE award) and GlaxoSmithKline for financial support, the EPSRC Mass Spectrometry Centre and the National Crystallography Service [University of Wales (Swansea) (HRMS) and University of Southampton (data sets)], Dr. Shane Sellarajah (UEA) for preliminary experiments and procedures for CSR experiments, Colin MacDonald (UEA) for VT NMR experiments, and Dr. Adrian G. Bateman, Dr. Bryan J. Davies, Dr. Kathy S. Harwood of Strategic Technologies, and Dr. Barbara O'Reilly of Analytical Sciences at GlaxoSmithKline for assistance with the Anachem SK233 system and chiral HPLC.

Supporting Information Available: Procedures for ee measurements of **2** and **4**; synthesis and characterization data for **3** and **4**; ¹H NMR spectra of **1** between –20 and 80 °C; and X-ray crystallographic details for (*P*)-**1**, (*M*)-**1**, and *rac*-**3**. This material is available free of charge via the Internet at <http://pubs.acs.org>.

OL0606132